

Asbestiform Chain Silicates: New Minerals and Structural Groups

Amphibole-mica intermediates exhibit both
structural order and disorder.

David R. Veblen, Peter R. Buseck, Charles W. Burnham

The pyroxenes, amphiboles, and micas are rock-forming silicate mineral groups of great interest to petrologists and mineralogists. They are widespread in the earth's crust, one or more of them occurring in almost all igneous and metamorphic rocks. They are also important in the upper mantle, where pyroxenes are a major component and where amphiboles and micas may be the most abundant hydrous minerals. Nearly all stony meteorites and lunar rocks contain pyroxenes.

The crystal structures of common pyroxenes, amphiboles, and micas were determined nearly 50 years ago. These structures are relevant not only for the geologist, but also for the solid-state chemist, since amphibole and mica may be considered as crystallographic shear structures derived from pyroxene (1, 2). Numerous excellent crystal structure refinements in recent years have yielded a detailed understanding of their crystal chemistry but have brought few surprises.

It is rather startling, considering the intensity with which the pyroxenes, amphiboles, and micas have been studied, that two new groups of chain silicates that are chemically and structurally intermediate between the amphiboles and micas were discovered in 1975 by standard single-crystal x-ray diffraction techniques (3). It is perhaps even more surprising that, since the initial discovery,

similar phases have been recognized in several other localities, suggesting that they may be relatively common features of certain geological environments. However, it is not geographical distribution that makes the new minerals particularly significant for the geological sciences, but rather their close relationships to the pyroxenes, amphiboles, and micas.

The new ordered structures provide additional information on the comparative crystal chemistry of the basic silicate structure types. Of equal importance may be the disordered states that coexist with the ordered structures and that contain information about reactions among the chain and sheet silicates. These disordered structures should also alert us to the possibility that pyroxenes and amphiboles can experience similar structural disorder and attendant chemical changes. In addition, the new phases show why some amphiboles can occur in either massive or fibrous forms, a dichotomy that has long been puzzling to mineralogists. Moreover, the structural nature and definition of amphibole asbestos are currently questions of great concern. Fibrous amphiboles are present in many rocks and are known to be released into the environment. In view of the health hazard posed by asbestos, a knowledge of the structural properties of these minerals should provide insight into a very important environmental problem.

Biopyribole Structures

The word biopyribole was first used in 1911 by Johannsen (4) as a collective name for the micas, pyroxenes, and amphiboles. He derived the term from *biotite* (a mica), *pyroxene*, and *amphibole*. The word has been used more recently in structural discussions of these mineral groups (5, 6). Since the new structures to be described in this article belong to the same structural family as these common groups, we will also adopt the collective term biopyribole to describe the pyroxenes, amphiboles, new minerals, and micas; we will use pyribole to describe the biopyriboles excluding the micas.

An understanding of the new minerals must be based on a knowledge of the classical biopyribole structures. We will therefore first describe the common pyroxene, amphibole, and mica structures and the history of their structure determinations. It would be difficult to overstate the importance of this early structural work for mineralogy, petrology, and crystal chemistry. Not even the generalized amphibole chemical formula was known before 1929, although the formula that was in use clearly disagreed with the analytical data. Until the structures were known, there was little rational basis for the distinction between amphiboles and pyroxenes, but it was immediately apparent from the structures that they are fundamentally different, although they possess certain structural similarities.

Classical Biopyriboles

Within the pyroxene and amphibole groups there is great chemical diversity but structural similarity. Since they are observed to be either orthorhombic or monoclinic, the pyroxenes and amphiboles are divided into ortho- and clino-subgroups. Each subgroup, in turn, contains numerous mineral species having

David Veblen is a research associate and Peter Buseck is a professor in the Departments of Geology and Chemistry, Arizona State University, Tempe 85281. Charles Burnham is a professor in the Department of Geological Sciences, Harvard University, Cambridge, Massachusetts 02138.

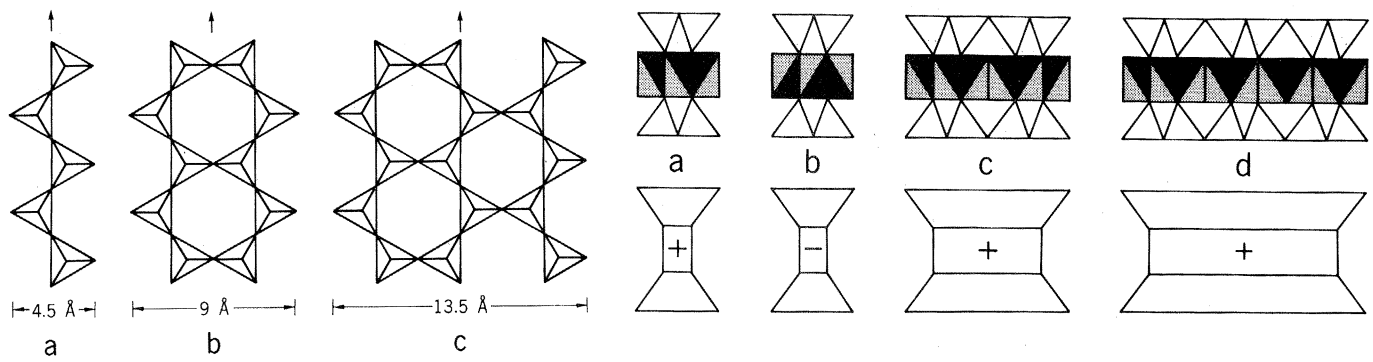


Fig. 1 (left). Silicate chains formed by oxygen sharing among SiO_4^{4-} tetrahedra. (a) Single chain, as found in pyroxenes. (b) Double chain, as found in amphiboles. (c) Triple chain, as found in the new minerals. The tetrahedral vertices represent oxygen atoms. Arrows indicate the chain directions (parallel to the c -axes); the indicated chain widths equal $\frac{1}{2}b$. Fig. 2 (right). Pyribole I-beams and their simplified representations, viewed parallel to the chains. Each I-beam consists of two silicate chains connected by shared oxygens to a strip of octahedrally coordinated cations. (a) Pyroxene I-beam in the (+) orientation. (b) Pyroxene I-beam in the (-) orientation. (c) Amphibole I-beam. (d) Triple-chain I-beam.

different mineral names. For example, diopside is a clinopyroxene with a specified range of composition; the structures of all other clinopyroxenes are topologically identical to that of diopside, since they can be produced simply by distortion of the diopside coordination polyhedra.

Clinopyroxene. The structure of diopside, approximately $\text{CaMgSi}_2\text{O}_6$, was determined in 1928 by Warren and Bragg (7), who used an elegant reductive method employing both symmetry and x-ray intensity information. It was shown that diopside contains silicon atoms coordinated by four oxygens in tetrahedral configuration. Oxygens are shared among these tetrahedra in such a way that they form continuous single silicate chains (Fig. 1). The chains are connected to each other by octahedrally coordinated magnesium and 8-coordinated calcium. Figure 2a shows a pyroxene module, or "I-beam," viewed parallel to the chains. The I-beam consists of two single chains connected by the octahedrally coordinated cations. (The "half" octahedra in

Fig. 2 are behind and partially hidden by the "whole" octahedra.) A simplified representation of the I-beam is also shown.

Clinoamphibole. Warren (8) derived the structure of the amphibole tremolite from that of diopside in 1929. He observed that the only major difference in the unit cell dimensions of diopside and tremolite is in the length of the b -axis: diopside has $b \approx 9$ angstroms, twice the width of the silicate chain, while in tremolite $b \approx 18$ angstroms (Table 1). Furthermore, the intensity distributions from the crystal planes defined by the indices ($h0\ell$) in tremolite and diopside are nearly identical, indicating that projections of their structures on to the (010) plane are almost the same. Since x-ray and etch-pit data showed that tremolite contains mirror planes normal to b , Warren simply inserted mirrors into the diopside structure to produce double silicate chains (Fig. 1b). X-ray intensity data confirmed this structure for tremolite, in which the silicate chains are again connected by Ca and Mg to form I-beams.

Figure 2c shows one of these amphibole I-beams and its simplified representation, viewed parallel to the chain direction.

The determination of the diopside and tremolite structures provided several new insights into the biopyribole family. The structures showed that the accepted diopside formula $\text{CaMgSi}_2\text{O}_6$ is correct but that tremolite is $\text{Ca}_2\text{Mg}_5\text{Si}_8\text{O}_{22}(\text{OH})_2$, not $\text{CaMg}_3(\text{SiO}_3)_4$ as had been thought. They also explained the different and diagnostic cleavages of the amphiboles and pyroxenes. Perhaps most important, the structures provided a rational basis for defining the pyroxenes and amphiboles: the pyroxenes contain single silicate chains, while the amphiboles have double silicate chains.

Orthopyroxene. In 1930, Warren and Modell (9) presented the structure of enstatite, $\text{Mg}_2\text{Si}_2\text{O}_6$. Noting that the cell dimensions differ from those of diopside primarily in the doubling of the a -axis (Table 1) and that the enstatite space group requires a b -glide plane parallel to (100), they derived the enstatite struc-

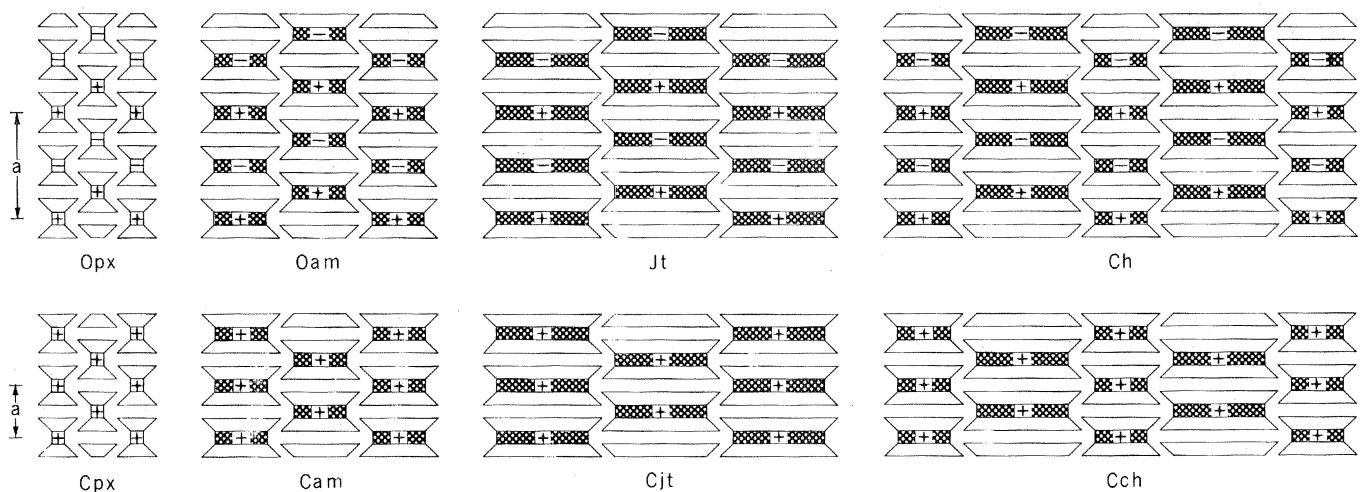


Fig. 3. I-beam diagrams showing the stacking sequences of orthopyroxenes (*Opx*), clinopyroxenes (*Cpx*), orthoamphiboles (*Oam*), clinoamphiboles (*Cam*), jimthompsonite (*Jt*), clinojimthompsonite (*Cjt*), chesterite (*Ch*), and the monoclinic analog of chesterite (*Cch*).

ture by "twinning" diopside on a unit-cell scale with a *b*-glide operation. They substantiated their structure with x-ray intensity measurements, establishing the orthopyroxenes as "true members of the pyroxene group" (9).

The primary difference between the clinopyroxene and orthopyroxene structures can be viewed in terms of the stacking of the I-beams in the *a* direction. I-beams oriented like the one in Fig. 2a can be distinguished from those oriented like the one in Fig. 2b. The two different orientations can be represented by (+) and (-), as shown. The sequence of I-beam orientations is called the "stacking sequence" of a pyribole; it can be described by listing the sequence of signs in the *a* direction. Figure 3 shows I-beam diagrams for the clinopyroxene and orthopyroxene structures. In clinopyroxene, the stacking sequence is (+++ etc.), or simply (+), indicating that all the I-beams are oriented in the same way. The same sequence also occurs in the clin amphiboles. The orthopyroxene stacking is different, (+-+-), and results in the doubling of *a*. A third variation, (+-), is found in some high-temperature phases (protoenstatite and protoamphibole) (10). Disordered stacking sequences and intergrowths of the several types are common in magnesium-rich pyroxenes (11).

Orthoamphibole. The structure of anthophyllite, $Mg_7Si_8O_{22}(OH)_2$, was reported in 1930 by Warren and Modell (12). The cell dimensions (Table 1) suggest close relationships with the previously solved pyribole structures; *a* is the same as in orthopyroxene, while *b* is the same as in clin amphibole. It was postulated that anthophyllite contains double chains like those of tremolite, with a stacking sequence like that of enstatite. In the words of Warren and Modell (12), "The cross connection between the four groups of pyroxenes and amphiboles is such a close one that the structure of anthophyllite could be derived in either of two ways: (1) anthophyllite is related to enstatite in the same way that tremolite is related to diopside, (2) anthophyllite could be derived from the tremolite structure by the same method that was used in deriving the enstatite structure from that of diopside." A detailed model was derived by introducing mirrors into the enstatite structure, and x-ray intensity data showed that it was correct.

Micas. The basic mica (13) structure types were guessed by Pauling (14) in 1930. His hypotheses were derived from Pauling's rules, cell dimensions, knowledge of some related structures, and the chemical and physical properties of the

minerals. These mica group minerals all contain sheets of silicate tetrahedra that are continuous in two dimensions (Fig. 4a). Pairs of sheets are joined together by octahedral cations to form "sandwiches" (Fig. 4b), which are stacked to form the three-dimensionally continuous structures. Large, ideally 12-coordinated sites between the sandwiches can be empty (talc, pyrophyllite), filled with monovalent cations (biotite, muscovite), or filled with divalent cations (clintonite, margarite). In real micas, distortion of the silicate sheets reduces the coordination number of these large sites to 6.

The detailed structure of muscovite, published by Jackson and West (15) in 1931, confirmed Pauling's guess. In addition, Jackson and West pointed out important structural relationships among the pyroxenes, amphiboles, and micas: the mica structure could be derived by repeating the process used to derive the amphibole structures from the pyroxene structures. It was realized that there is a logical polymerization series from single chains to double chains to sheets, and that the biopyriboles comprise a closely related family, both structurally and chemically.

New Biopyriboles

The new minerals were found near Chester, Vermont, where they occur with talc (a mica) and anthophyllite, cummingtonite, and tremolite (amphiboles) (16). They were first recognized by the long *b*-axes of their unit cells, as observed on x-ray precession photographs. Table 1 shows the unit-cell parameters, compared with those of pyroxenes and amphiboles. The similarities in *a* and *c* dimensions are striking, and all *b* dimensions are approximate multiples of 9 Å. By comparing Fig. 1 and Table 1, it can be seen that the length of the *b*-axis in pyroxene is twice the width of a single chain, and in amphibole it is twice the width of a double chain. These data therefore suggest that the new minerals differ from the classical pyriboles primarily in the widths of their silicate chains and the octahedral strips to which they are attached. The (*h0l*) intensity distributions are nearly identical to those of pyroxenes and amphiboles, supporting the notion that the new minerals are pyriboles as well.

The unit-cell dimensions and space groups suggest that two of the new min-

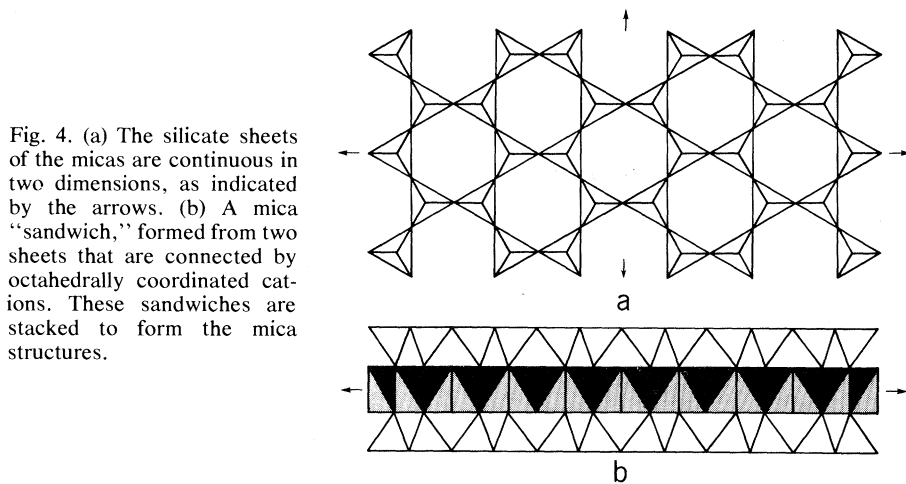


Fig. 4. (a) The silicate sheets of the micas are continuous in two dimensions, as indicated by the arrows. (b) A mica "sandwich," formed from two sheets that are connected by octahedrally coordinated cations. These sandwiches are stacked to form the mica structures.

Table 1. Pyribole cell parameters and space groups.

Group	System	Cell parameters				Space group
		<i>a</i> (Å)	<i>b</i> (Å)	<i>c</i> (Å)	β (deg)	
Pyroxene						
Enstatite (9)	Orthorhombic	18.2	8.86	5.20		<i>Pbca</i>
Diopside (7)	Monoclinic	9.71	8.89	5.24	105.8	<i>C2/c</i>
Amphibole						
Anthophyllite (12)	Orthorhombic	18.5	17.9	5.27		<i>Pnma</i>
Tremolite (8)	Monoclinic	9.78	17.8	5.26	106.0	<i>C2/m</i>
New						
Jimthompsonite	Orthorhombic	18.63	27.23	5.30		<i>Pbca</i>
Clinojimthompsonite	Monoclinic	9.87	27.24	5.32	109.5	<i>C2/c</i>
Chesterite	Orthorhombic	18.61	45.31	5.30		<i>A2₁ma</i>
Unnamed	Monoclinic	9.87	45.31	5.29	109.7	<i>A2/m, A2, Am</i>

erals, jimthompsonite and clinojimthompsonite (17), contain triple silicate chains, as shown in Fig. 1c. The triple chains are connected to wide octahedral strips to form I-beams, just as in the pyroxenes and amphiboles (Fig. 2d). In jimthompsonite these I-beams are stacked like those of orthopyroxenes and orthoamphiboles (+ + - -), and in clinojimthompsonite they are stacked like those of clinopyroxenes and clinoamphiboles (+). These model structures are shown schematically in Fig. 3. The observed space groups, *Pbca* and *C2/c* (or *Cc*), are consistent with these models and are the same as the enstatite and diopside space groups.

Two of the three space groups that are consistent with the diffraction symbol of the third new mineral, chesterite, are inconsistent with pyribole symmetry operations. The remaining group, *A2₁ma*, permits a model that contains both double and triple silicate chains, alternating rigorously in the *b* direction, and that possesses the (+ + - -) stacking of orthopyroxenes and orthoamphiboles. The three possible space groups of the monoclinic analog of chesterite are all consistent with an alternating chain model having the clinopyroxene-clinoamphibole (+) stacking sequence. These models are shown schematically in Fig. 3.

Structure refinements. A detailed structural model for jimthompsonite was derived by extending the orthopyroxene structure in the *b* direction, just as Warren and Modell derived anthophyllite from enstatite and tremolite from diopside. The clinojimthompsonite model was derived from the refined jimthompsonite structure, employing the reverse of the transformation that Warren and Modell used to derive enstatite from diopside. Finally, the chesterite model was calculated by joining a unit of jimthompsonite structure to one of anthophyllite. A detailed structural model of the monoclinic polymorph of chesterite could be derived by applying the enstatite-diopside type of transformation to the refined chesterite structure.

Least-squares refinement of these models, using three-dimensional x-ray intensity data, resulted in unweighted reliability indices between 0.067 and 0.084, and weighted indices between 0.045 and 0.057 (18). For all refinements we utilized isotropic temperature factors and varied octahedral site occupancies, assuming full occupancy by Mg and Fe. The structures were confirmed by Fourier electron density difference maps after completion of the refinements. The structure of the monoclinic polymorph of chesterite has not been refined, but its relations to the chesterite structure strongly suggest that the proposed model is correct.

Triple silicate chains are known to occur in only two substances other than these biopyriboles from Chester. Synthetic $\text{Ba}_4\text{Si}_6\text{O}_{16}$ contains triple chains, but they are different from those in the Chester minerals (Fig. 1c) because the apical oxygens in adjacent tetrahedra point in opposite directions (19). The structure of a synthetic hydrous NaMg silicate with triple chains has been solved using electron diffraction intensities (20). This phase is isostructural with clinojimthompsonite, suggesting that the new minerals from Chester could have natural analogs containing octahedrally coordinated cations other than Mg and Fe. Chesterite is apparently the first known example of a mixed-chain silicate—one containing more than one topologically distinct type of chain.

Chemistry. Electron microprobe analyses of crystals identified optically or by x-ray diffraction support the ideal structural formulas for the new minerals: $(\text{Mg,Fe})_{10}\text{Si}_{12}\text{O}_{32}(\text{OH})_4$ for jimthompsonite and clinojimthompsonite and $(\text{Mg,Fe})_{17}\text{Si}_{20}\text{O}_{54}(\text{OH})_6$ for chesterite, with small amounts of Mn and Ca substituting for Mg and Fe (18). The compositions (Fig. 5) are colinear with those of enstatite, clinoenstatite, anthophyllite, cummingtonite, and talc. The colinearity is a direct result of the structural relationships among the biopyriboles that have been elucidated by Thompson (5,

6); if ideal pyroxene and mica structures are cut into slabs parallel to (010) and combined in a 1:1 ratio, the result is an amphibole structure. These pyroxene and mica slabs can be combined in other ratios and sequences to produce triple-chain pyriboles, mixed double-triple chain pyriboles, and so on. Thompson (21) used this relationship to predict the existence of the jimthompsonite structure in 1971, 4 years before its discovery.

Structurally Disordered States

During the x-ray part of this study, the diffraction photographs of many of the "single crystals" that were examined indicated that they are multiphase mixtures of amphibole and the new pyriboles; diffuse streaks parallel to the reciprocal lattice axis *b** further suggested that some crystals are structurally disordered in the *b* direction. Presumably, these crystals possess (i) many mistakes in the sequence of double and triple chains, (ii) regions of no apparent order in the chain sequence, or (iii) areas with chains even wider than triple. When observed in a light microscope, the disordered regions are streaked parallel to (010). (See cover photo.) To establish the nature of the structural disorder, we initiated a high-resolution transmission electron microscope (HRTEM) study to observe directly the chain sequences. Similar methods have previously permitted characterization of structural disorder in other minerals (11, 22), and in one study scattered triple chains were imaged in several amphiboles (anthophyllite, tremolite, and amosite) (23).

High-resolution microscopy. The HRTEM study was conducted on a slightly modified JEM 100B microscope (24). Specimens were prepared by three different methods: (i) grinding and deposition onto holey carbon grids, (ii) microtoming epoxy-embedded specimens with a diamond knife, and (iii) ion-thinning crystals from petrographic thin sections. Similar results were obtained with all these methods, demonstrating that the observed effects were not produced during sample preparation but during the metamorphic and deformational events that occurred in southeastern Vermont.

The HRTEM investigation of the disordered phases requires that the double- and triple-chain portions of the structure produce distinctive contrast in the multiple-beam bright-field images. Recognition of double- and triple-chain contrast was achieved by correlating images of the known, rigorously ordered structures with their diffraction patterns. Im-

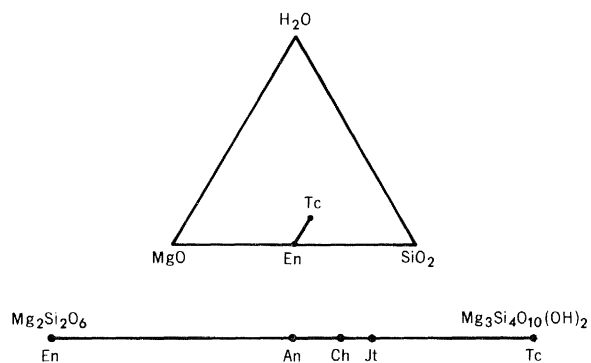


Fig. 5. Idealized compositions of the Mg biopyriboles enstatite and clinoenstatite (*En*), anthophyllite and cummingtonite (*An*), chesterite (*Ch*), jimthompsonite and clinojimthompsonite (*Jt*), and talc (*Tc*), shown on a binary composition diagram. The location of this binary join is shown above, on the ternary $\text{MgO-SiO}_2\text{-H}_2\text{O}$ diagram.

ages projected down the *a*-axis have readily recognizable and interpretable contrast, with sharp dark fringes marking the chain edges when the electron microscope is underfocused about 1000 Å. Figure 6, a and b, illustrates the contrast produced by double chains (anthophyllite) and triple chains (jimthompsonite). The alternation of these types of contrast in chesterite (Fig. 6c) supports the validity of this interpretation of the fringes observed with the electron microscope.

HRTEM results. Examination of many crystals has shown that structural disorder is widespread in the Chester chain silicates, ranging from isolated faults in otherwise well-ordered crystals to re-

gions with apparently random chain sequences. Figure 7, a and b, illustrates the former case; otherwise ordered anthophyllite and jimthompsonite crystals are interrupted by solitary chains of the wrong width. Figure 7c, on the other hand, is an image from a crystal with no apparent ordering scheme.

It was expected that the HRTEM study might reveal silicate chains wider than triple. Quadruple and quintuple chains, analogous to the triple chains in $\text{Ba}_4\text{Si}_6\text{O}_{16}$, occur in $\text{Ba}_3\text{Si}_8\text{O}_{21}$ and $\text{Ba}_6\text{Si}_{10}\text{O}_{26}$, respectively (19), as does local chain-width disorder (25). Figure 8 shows an *a*-axis photograph of a section of biopyribole chain silicate from Ches-

ter, containing what we interpret to be quadruple and septuple chains. To date, no structurally ordered phases with chains wider than triple have been observed, but this study is not yet complete, and regions containing high concentrations of quadruple and wider chains have been observed. Furthermore, we have observed what we interpret to be chains of width 5, 6, 7, 8, . . . , including chains with widths up to 60 pyroxene chains. It is an arbitrary distinction whether these should be called chains or finite sheets, since the interiors of these wide chains are talclike.

Some ordered chain sequences other than those found in the x-ray study ap-

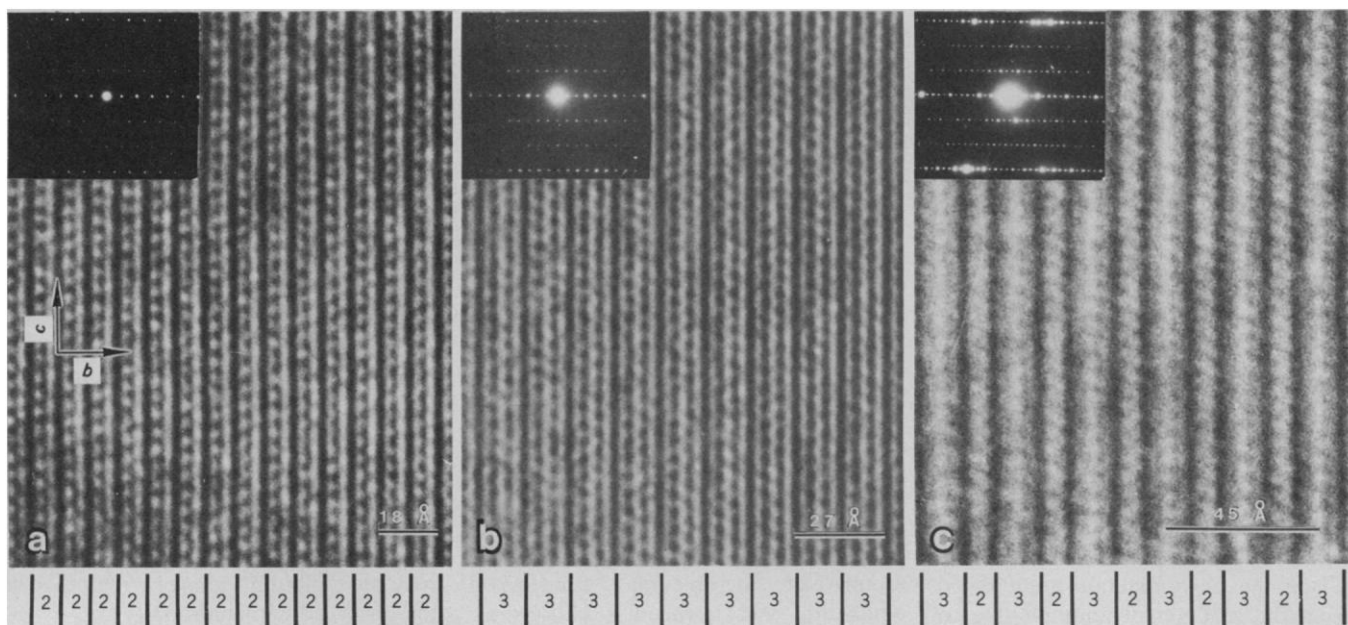


Fig. 6. HRTEM *a*-axis images and electron diffraction patterns of ordered pyriboles: (a) anthophyllite (double chains), (b) jimthompsonite (triple chains), and (c) chesterite (alternating double and triple chains). Dark fringes mark the chain edges; variations in detailed contrast result from variations in microscope operating conditions. The axial directions *b* and *c* are the same for all the minerals, and all subsequent figures are in the same orientation.

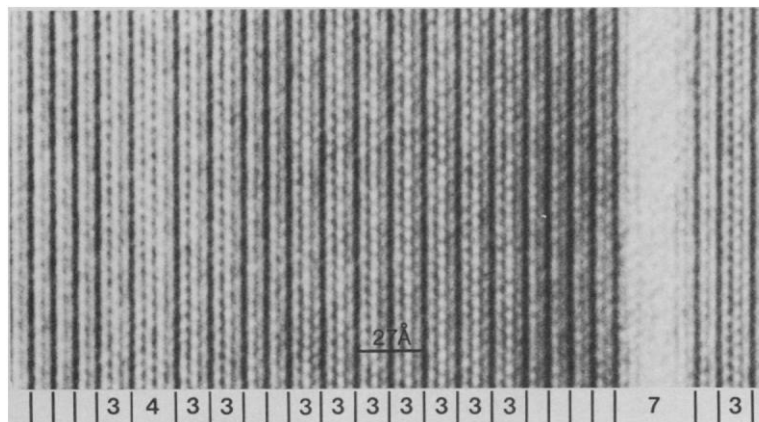
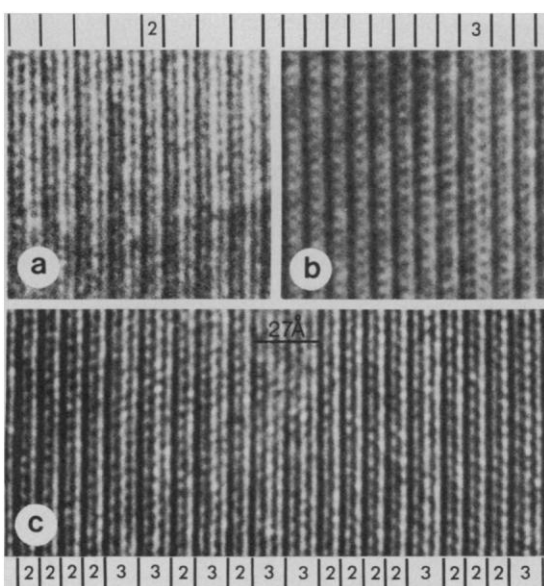


Fig. 7 (left). (a) Isolated double chain ("2") in jimthompsonite. (b) Isolated triple chain ("3") in anthophyllite. (c) Disordered sequence of double and triple chains ("2" and "3," respectively). This and subsequent figures can best be viewed at a low angle, parallel to the chains. Fig. 8 (right). Quadruple ("4") and septuple ("7") chains in pyribole from Chester. Double chains are not labeled.

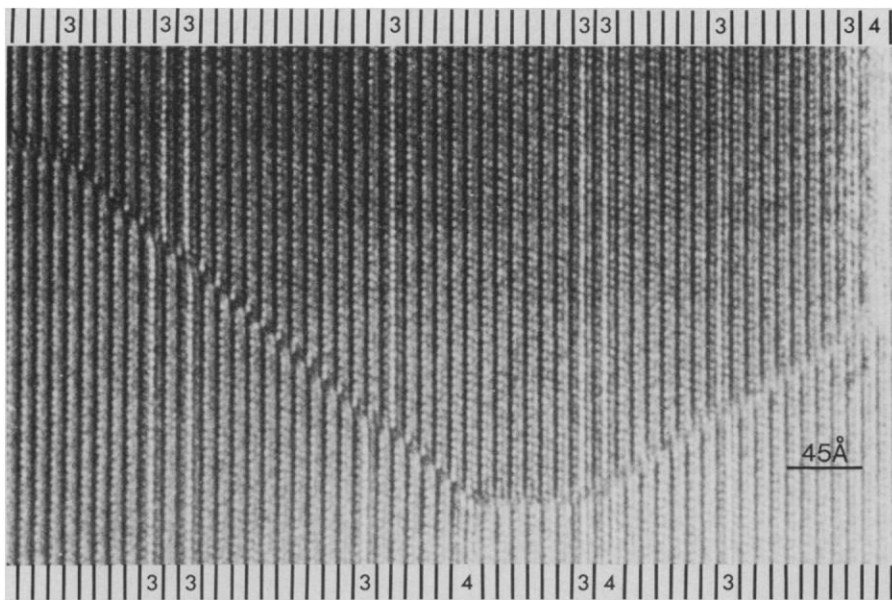


Fig. 9. Low-angle fault in anthophyllite with terminating triple ("3") and quadruple ("4") chains. Since the triple chains are not rigorously related across the fracture, they must have grown after the fault formed.

pear to occur with greater than random frequency. For example, a perfectly ordered structure in which pairs of double chains alternate with pairs of triple chains has been found occurring as (010) lamellae up to 700 Å wide. Further observations are required to determine which of the observed sequences are statistically significant.

Amphibole-Mica Reaction

Since the new minerals are created during the reaction of anthophyllite to form talc, they provide insight into the amphibole-mica reaction pathways. The mechanism of this reaction is not simple. Rather than only one step, it is now clear that a sequence of structurally disordered and ordered states is involved in this reaction, at least as it occurred in the rocks at Chester. It is not clear, however, whether all crystals that are reacting to form talc assume the chesterite and jimthompsonite structures, but these ordered structures certainly must be intermediate phases representing local free energy minima in the compositional path of the reaction. Considering the kinetic difficulties that have been encountered in experimental studies of anthophyllite stability (26), it would probably be very difficult even to determine reliably whether the new ordered structures have fields of stability or are metastable. Furthermore, we have examined several synthetic anthophyllites used in stability studies; all are structurally disordered, in some cases consisting of intimate mixtures of chains of many widths.

Before the HRTEM study, it was considered likely that triple chains in anthophyllite would always be found in even multiples, such as pairs, since by a simple shearing mechanism three double-chain I-beams (see Fig. 2) may be converted to two triple-chain I-beams with minimal diffusion of H⁺ and octahedral cations. Although triple chains are commonly paired, isolated triple chains are by no means uncommon (Fig. 7a). The growth of a triple-chain I-beam from either one or two double-chain I-beams requires considerable mass transfer of octahedral and tetrahedral cations as well as oxygen anions.

Low-angle faults and chain terminations. Figure 9 shows part of a crystal

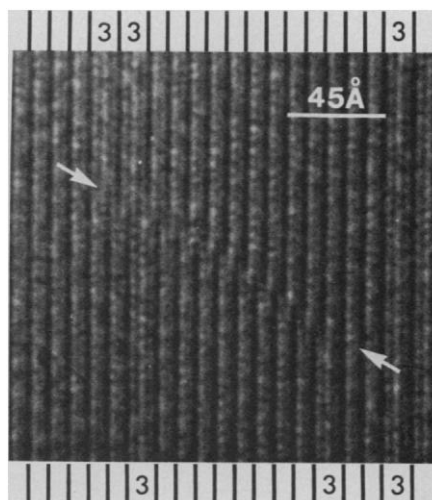


Fig. 10. Triple chains ("3") terminating in amphibole structure. The terminations are coupled and connected by a planar fault, which lies between the arrows.

that contains a low-angle grain boundary (about 1° rotation), probably created when the crystal was broken during deformation of the host rock. Since the triple chains growing in the predominant amphibole structure are not rigorously related to each other across the boundary, we can infer the following sequence of geological events from this crystal: (i) prograde metamorphism, during which the original amphibole crystal grew; (ii) deformation of the rock, causing the crystal to break; and (iii) retrograde metamorphism, during which triple and quadruple chains grew independently on either side of the break. This sequence is consistent with data on rolled garnets from the mantled gneiss domes of southeastern Vermont; the garnet data show that at least two deformational events occurred during the Acadian metamorphism (27).

Terminations of individual chains have also been observed in some crystals. Figure 10 shows two triple chains terminating in the amphibole structure and connected by a planar fault with a projected displacement of one-fourth the amphibole *b* dimension. In all cases where they have been seen, the terminations of at least two chains are coupled in a similar manner. These paired terminations could have arisen in at least two ways: (i) one unit of triple-chain structure may have "derailed" during growth and continued to grow in the offset position or (ii) two triple chains growing simultaneously from opposite directions may have met and pinned each other in the observed configuration.

Amphibole Asbestos

Fine-grained, airborne asbestos particles have been shown to cause a variety of lung diseases, including cancer and asbestosis (28), and some forms of asbestos may be toxic when ingested (29). The Reserve Mining case (30) has dramatically shown that asbestos pollution can result from operations unrelated to asbestos mining and use. Since fibrous amphiboles are common minor constituents of many rocks, asbestos pollution may be a side effect of numerous mining and quarrying operations, suggesting that it will remain an important health problem in the future (31). Moreover, asbestos is used in a wide variety of applications in manufacturing and construction industries and is contained in many products found in the home.

Asbestos can be subdivided into two major categories: (i) chrysotile, a serpentine mineral, and (ii) amphibole asbestos.

Although chrysotile accounts for about 95 percent of commercial asbestos, amphibole asbestos can still enter the environment in massive amounts and must therefore be considered a health hazard. Amphibole asbestos has been extensively studied, but it has never been fully explained why some amphiboles can occur in either fibrous or nonfibrous forms. Chisholm (2) speculated that the fibrous habit might result from structural faults. We believe that the structural details presented in this article may help to resolve this problem: amphiboles break not only along their normal cleavage and twin planes but also along chains of anomalous width, and the latter type of break causes them to be fibrous. Thus, amphiboles with many errors in chain width will be fibrous, while those without such errors will be massive. The intergrowths of biopyriboles from Chester exhibit (010) partings, which could arise by breaking along chains of the wrong width, and (100) partings, which may result from breaking along twin planes or stacking faults. These minerals are typically fibrous when crushed.

Errors in chain width have been noted in several fibrous amphiboles (23; this study) but have not been reported in nonfibrous amphiboles. For example, a fibrous tremolite studied by Hutchison *et al.* (23) contains some triple chains, whereas we observed only double chains in a massive tremolite. Similarly, the fibrous orthoamphibole from Chester contains high concentrations of chains of the wrong width, which were not observed in a nonfibrous orthoamphibole that we studied from another locality. This suggests that the presence of chain width errors will prove to be a common denominator of all amphibole asbestos.

If the fibrous nature of amphibole asbestos does result from chain width errors, as suggested above, then such asbestos cannot strictly be considered to be amphibole at all; instead, the compositions will fall in biopyribole compositional space, off the amphibole composition. Possibly some amphibole asbestos should be called chesterite or jimthompsonite asbestos, since these new minerals are also fibrous. Indeed, much asbestos may turn out to exhibit extreme structural disorder and thus may elude any simple classification. Considering the present ambiguities, we suggest that the term *pyribole asbestos* be used, as this would encompass all these possibilities while still distinguishing these materials from chrysotile.

Much additional work will be needed before the problems surrounding pyribole asbestos are resolved. Future study

must include both chemical and structural characterization. It has recently become possible to obtain quantitative chemical analyses from small unpolished particles (32), and this article demonstrates that single-crystal x-ray and HRTEM methods can be used together to solve complex structural problems. Detailed knowledge of ordered structures can be derived from x-ray studies and is needed for correct interpretation of electron imaging results. For particles too small to use in single-crystal x-ray studies, electron diffraction patterns from single crystals in critical orientations are helpful; streaking parallel to a^* indicates errors in the stacking sequence of I-beams or fine-scale twinning, while streaking parallel to b^* arises from chain width disorder. The most detailed knowledge of defect structures can be obtained by using HRTEM imaging, which provides small-scale information inaccessible to x-ray methods. Since the physical properties of pyribole asbestos apparently depend on defects, HRTEM study will be necessary for full characterization of these materials.

Summary

The discovery and characterization of structurally ordered and disordered phases that are intermediate between amphiboles and micas have shown that the biopyriboles are a much more complex family of minerals than has previously been recognized. In addition to single-chain, double-chain, and sheet structures, there are also minerals with triple chains and with alternating double and triple chains. Many crystals exhibit disorder in the sequence of double and triple chains, and isolated chains that are wider than triple are common. This structural disorder helps to explain why asbestiform amphiboles are fibrous.

The new phases have now been found in several localities, and it is possible that similar phenomena in other minerals could also have been overlooked. In particular, there is no reason to suppose that analogous substances and structures with both single and double chains do not occur between the pyroxenes and the amphiboles. Since the pyroxenes are used extensively by geologists to assess rock histories and formation temperatures and pressures, it is essential that the extent of this type of disorder be evaluated. It is possible that what appears to be only an interesting mineralogical problem may prove to be a petrological nightmare.

References and Notes

1. A. D. Wadsley and S. Andersson, in *Perspectives in Structural Chemistry*, J. D. Dunitz and J. A. Ibers, Eds. (Wiley, New York, 1970), vol. 3, pp. 1-58.
2. J. E. Chisholm, *J. Mater. Sci.* **8**, 475 (1973).
3. D. R. Veblen and C. W. Burnham, *Eos* **56**, 1076 (1975); *Geol. Soc. Am. Abstr. Programs* **8**, 1153 (1976); D. R. Veblen, thesis, Harvard University (1976).
4. A. Johannsen, *J. Geol.* **19**, 317 (1911).
5. J. B. Thompson, *Am. Mineral.* **55**, 292 (1970).
6. ———, in preparation.
7. B. E. Warren and W. L. Bragg, *Z. Kristallogr.* **69**, 168 (1928).
8. B. E. Warren, *ibid.* **72**, 42 (1929).
9. ——— and D. I. Modell, *ibid.* **75**, 1 (1930).
10. J. R. Smyth and J. Ito, *Eos* **58**, 312 (1977); G. V. Gibbs, in *Mineral. Soc. Am. Spec. Pap.* **2** (1969), p. 101.
11. S. Iijima and P. R. Buseck, *Am. Mineral.* **60**, 758 (1975); P. R. Buseck and S. Iijima, *ibid.* p. 771; S. Iijima and P. R. Buseck, in *Electron Microscopy in Mineralogy*, H.-R. Wenk, Ed. (Springer-Verlag, Berlin, 1976), pp. 319-323.
12. B. E. Warren and D. I. Modell, *Z. Kristallogr.* **75**, 161 (1930).
13. The term mica is often applied only to mica group minerals having monovalent interlayer cations. In this article we apply it to the entire group, without regard to the presence or oxidation state of interlayer cations.
14. L. Pauling, *Proc. Natl. Acad. Sci. U.S.A.* **16**, 123 (1930).
15. W. W. Jackson and J. West, *Z. Kristallogr.* **76**, 211 (1931).
16. The new minerals occur in the blackwall reaction zone surrounding a metamorphosed ultramafic body on the west limb of the Chester dome.
17. The mineral names jimthompsonite, clinojimthompsonite, and chesterite have been approved by the International Mineralogical Association Commission on New Minerals and Mineral Names. The fourth new phase is unnamed, though it bears an obvious relationship to chesterite.
18. A paper describing physical, optical, and chemical properties and geological occurrence and a second paper discussing structure refinements, bond distances and angles, and the crystal chemistry are in preparation (D. R. Veblen and C. W. Burnham).
19. F. Liebau, in *Handbook of Geochemistry*, K. H. Wedepohl, Ed. (Springer-Verlag, Berlin, 1972), vol. 2, chap. 14, pp. A1-A32.
20. V. A. Drits, Yu. I. Goncharov, V. A. Aleksandrova, V. E. Khadzhi, A. L. Dmitrik, *Kristallografiya* **19**, 1186 (1974); translated in *Sov. Phys. Crystallogr.* **19**, 737 (1975).
21. J. B. Thompson, unpublished manuscript (1971), to appear in revised form (6).
22. S. Iijima and P. R. Buseck, *Acta Crystallogr. Sect. A*, in press; L. Pierce and P. R. Buseck, *Science* **186**, 1209 (1974).
23. J. L. Hutchison, M. C. Irusteta, E. J. W. Whittaker, *Acta Crystallogr. Sect. A* **31**, 794 (1975).
24. P. R. Buseck and S. Iijima, *Am. Mineral.* **59**, 1 (1974).
25. M. Czank and P. R. Buseck, in preparation.
26. H. J. Greenwood, *J. Petrol.* **4**, 317 (1963); K. L. Cameron, *Am. Mineral.* **60**, 375 (1975); R. K. Popp, M. C. Gilbert, J. R. Craig, *ibid.* **61**, 1267 (1976).
27. J. L. Rosenfeld, in *Studies of Appalachian Geology, Northern and Maritime*, E-an Zen, W. S. White, J. B. Hadley, J. B. Thompson, Eds. (Interscience, New York, 1968), pp. 185-202.
28. I. J. Selikoff, J. Churg, E. C. Hammond, *J. Am. Med. Assoc.* **188**, 22 (1964).
29. I. J. Selikoff, R. A. Bader, M. E. Bader, J. Churg, E. C. Hammond, *Am. J. Med.* **42**, 487 (1967).
30. J. P. Hills, *Environ. Sci. Technol.* **10**, 235 (1976); P. M. Cook, G. E. Glass, J. H. Tucker, *Science* **185**, 853 (1974).
31. A. N. Rohl, A. M. Langer, I. J. Selikoff, *Science* **196**, 1319 (1977); *ibid.* **197**, 716 (1977).
32. J. T. Armstrong and P. R. Buseck, *Anal. Chem.* **47**, 2178 (1975).
33. We warmly thank J. B. Thompson, Jr., for his help; many of the structural concepts presented here originated with him. The microscopy was performed at the electron microscope facility in the Center for Solid State Science at Arizona State University, where J. Wheatley was of assistance. X-ray work was supported by NSF grant GA-41415 to C.W.B., and electron microscopy and associated work was supported by grants EAR77-00128 and AENV76-17130 to P.R.B.